

MK-SGN: A Spiking Graph Convolutional Network with Multimodal Fusion and Knowledge Distillation for Skeleton-based Action Recognition

Naichuan Zheng

Beijing Laboratory of Advanced
Information Networks
Beijing Key Laboratory of Network
System Architecture and
Convergence
School of Information and
Communication Engineering
Beijing University of Posts and
Telecommunications
Beijing, China
2022110134zhengnaichuan@bupt.edu.cn

Hailun Xia*

Beijing Laboratory of Advanced
Information Networks
Beijing Key Laboratory of Network
System Architecture and
Convergence
School of Information and
Communication Engineering
Beijing University of Posts and
Telecommunications
Beijing, China
xiahailun@bupt.edu.cn

Zeyu Liang

Beijing Laboratory of Advanced
Information Networks
Beijing Key Laboratory of Network
System Architecture and
Convergence
School of Information and
Communication Engineering
Beijing University of Posts and
Telecommunications
Beijing, China
lzy_sfading@bupt.edu.cn

ABSTRACT

In recent years, skeleton-based action recognition, leveraging multimodal Graph Convolutional Networks (GCN), has achieved remarkable results. However, due to their deep structure and reliance on continuous floating-point operations, GCN-based methods are energy-intensive. To address this issue, we propose an innovative Spiking Graph Convolutional Network with Multimodal Fusion and Knowledge Distillation (MK-SGN). By merging the energy efficiency of Spiking Neural Network (SNN) with the graph representation capability of GCN, the proposed MK-SGN reduces energy consumption while maintaining recognition accuracy. Firstly, we convert GCN into Spiking Graph Convolutional Network (SGN) and construct a foundational Base-SGN for skeleton-based action recognition, establishing a new benchmark and paving the way for future research exploration. Secondly, we further propose a Spiking Multimodal Fusion module (SMF), leveraging mutual information to process multimodal data more efficiently. Additionally, we introduce a spiking attention mechanism and design a Spatio Graph Convolution module with a Spatial Global Spiking Attention mechanism (SA-SGC), enhancing feature learning capability. Furthermore, we delve into knowledge distillation methods from multimodal GCN to SGN and propose a novel, integrated method that simultaneously focuses on both intermediate layer distillation and soft label distillation to improve the performance of SGN. On two challenging datasets for skeleton-based action recognition, MK-SGN outperforms the state-of-the-art GCN-like frameworks in reducing computational load and energy consumption. Specifically, it achieves a top-1 accuracy of 78.5% on the NTU-RGB+D 60 cross-subject split using 4-time steps with the theoretical energy consumption of $0.614mJ$ per action sample. In contrast, typical GCN methods typically consume more than $35mJ$ per action sample, while MK-SGN reduces energy consumption by more than 98%.

CCS CONCEPTS

• **Computing methodologies** → **Activity recognition and understanding.**

KEYWORDS

Spiking Graph Convolution Network, Multimodal, Knowledge Distillation, skeleton-based Action Recognition

1 INTRODUCTION

Human action recognition is a crucial task with many applications [48], including human-robot interaction [39], video surveillance [10] and emergency detection [1]. The emergence of depth sensors and their robustness against complex backgrounds have recently drawn significant attention to skeleton-based action recognition [4, 18, 32, 43]. Currently, Graph Convolutional Networks (GCN), as a kind of Artificial Neural Networks (ANN), have achieved remarkable results [25, 35, 40]. The introduction of ST-GCN [53] marks the first attempt to represent skeletons through spatio-temporal relation, laying the foundation for numerous subsequent studies. Shift-GCN [5] makes advancements towards lightweight processing. Multimodal integration has proved beneficial in many fields because different models can provide complementary information that enhances overall understanding, decision-making accuracy, user experience, and system performance [2, 13]. Based on this understanding, recent methods train multiple unimodal GCNs to recognize human actions from various modalities of skeleton data, such as joint, bone, and motion [3, 7, 54]. Furthermore, the proposal of the multimodal foundation model, the HULK model, elevates the precision of skeleton-based action recognition to a new level [50]. However, GCN has high computational energy consumption when identifying skeletal actions, especially for multimodal data. For example, despite being touted for their lightweight designs, models such as Shift-GCN and CTR-GCN still consume considerable energy, requiring $46mJ$ and $36.25mJ$ per action sample when processing multimodal skeleton data. In comparison, the energy consumption of 2S-AGCN [41] escalates dramatically to $164.68mJ$ per action

*Corresponding Author

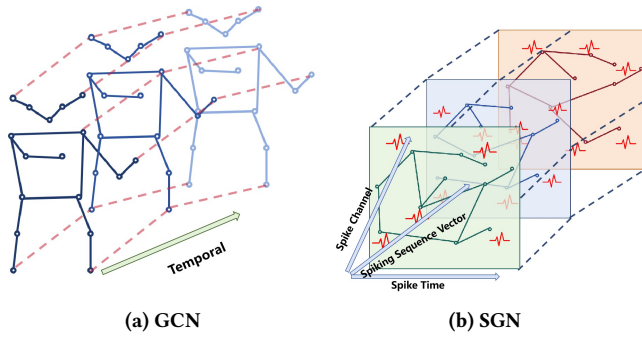


Figure 1: Comparison of GCN and SGN for skeleton-based Action Recognition. The former (a) performs feature extraction and information propagation on nodes of the graph structure through graph convolutional layers, while the latter (b) employs spike encoding to convert features into discrete spike-form, conducting feature extraction and information propagation in the time dimension of spike signals.

sample. Further details on the calculation of theoretical energy consumption for these models can be found in the discussion in Section 4.3.

As the third generation of neural networks [34], Spiking Neural Networks (SNN) originated from biomimetics and are renowned for their event-driven characteristics, which result in exceptionally low energy consumption [37, 46]. With the advancement of ANNs, SNNs have enhanced their performance by adopting advanced architectures [14, 15]. Examples include Spiking Graph Neural Networks [61], Spiking Recurrent Neural Networks [8, 47] and Spiking Transformers [56, 60], all of which have been subjected to substantial research. Current research in Spiking Neural Networks (SNNs) primarily focuses on the classification of RGB images and event-driven recognition [19, 45, 58], achieving notable results in reducing energy consumption while ensuring accuracy. Inspired by these successful examples, we are similarly motivated to explore skeletal action recognition based on Spiking Graph Convolutional Networks. This new investigation aims to leverage the efficiency of SNNs and the performance advantages of GCNs, bringing revolutionary progress to skeletal action recognition. Through this research, we hope to reduce energy consumption and expand the potential applications of SNNs in complex dynamic scenarios, ensuring high accuracy.

Several scientific challenges during this research process prompt deep reflection. First, given the complex graphical nature of skeletal data, how can we effectively convert it into spike signals? Furthermore, can spike-form data, transformed from graph data, be compatible with traditional GCN and function effectively in action recognition tasks? Facing complex multimodal data, how should we design strategies to achieve effective data fusion within SNN? Lastly, how can we achieve a trade-off between reducing energy consumption and maintaining recognition accuracy?

To tackle these issues, we first propose a spiking coding module to convert skeletal data into event spikes and devise a Base Spiking Graph Convolutional Network (SGN) for feature representation and classification. The difference between SGN and traditional Graph

Convolutional Networks (GCN) lies in feature extraction and information propagation, as shown in Figure 1. Secondly, we develop a multimodal spike data fusion module based on mutual information, utilising mutual information to compute the correlation between multimodal data for early fusion. Building upon this, we introduce a spiking spatial graph convolutional network based on spiking attention to process the fused spike-form feature. Thirdly, to ensure accuracy without increasing model complexity, we proposed a novel GCN-to-SGN knowledge distillation method, leveraging high-precision traditional GCN to guide the training of SGN. It implements the distillation of features from intermediate layers and soft labels. Ultimately, we propose a Spiking Graph Convolutional Network with MultiModal Fusion and Knowledge Distillation (MK-SGN) for skeleton-based action recognition. In summary, our work has three main contributions as follows:

- (1) We introduce skeleton-based action recognition into a new domain for the first time, using SGN for recognition. This leads to the establishment of a novel research domain and the corresponding benchmark model Base-SGN.
- (2) We propose a Spiking Multimodal Fusion (SMF) module for fusing multimodal data based on mutual information to reduce energy consumption while enhancing performance. We further incorporate a spatial global spiking attention mechanism into spatial graph convolutions to design a Spiking Graph convolution (SA-SGC) to enhance learning capability.
- (3) We propose a groundbreaking method of distilling knowledge of GCN-to-SGN. Our distillation method involves distilling intermediate features and soft labels. Inner layer distillation entails transforming multimodal GCN features into SGN features through a proposed Feature Translation Module (FTM). Soft label distillation combines the soft labels from the multimodal teacher GCN network.
- (4) Extensive experiments on two challenging datasets demonstrate the advantages of our work. The theoretical energy consumption of MK-SGN is $0.614mJ$ per action sample. Compared to the GCN-based methods, it reduces more than 98.5%.

2 RELATED WORK

In recent years, with the continuous advancement of deep learning, skeleton-based action recognition has become a highly focused research area. Early studies primarily focused on utilizing methods such as CNNs [6, 31] and RNNs [8, 30, 49], while the subsequent introduction of ST-GCN [29] represented skeletons as graphs, effectively capturing spatio-temporal relationships and achieving some success. Subsequently, many studies have focused on improving the performance of skeleton-based action recognition based on GCNs [12]. Some research emphasizes capturing global and local information, such as ASGCN [26], while others attempt to improve performance while reducing computational complexity, such as Shift-GCN [5]. With the deepening of research, multimodal skeleton data has begun to receive attention, including joint, bone and motion information, such as CTR-GCN [3] and Info-GCN [7]. In 2023, Hulk was proposed, leveraging multimodal pre-trained models to push skeleton-based action recognition to new heights [50]. However, these studies have almost exclusively focused on ANNs,

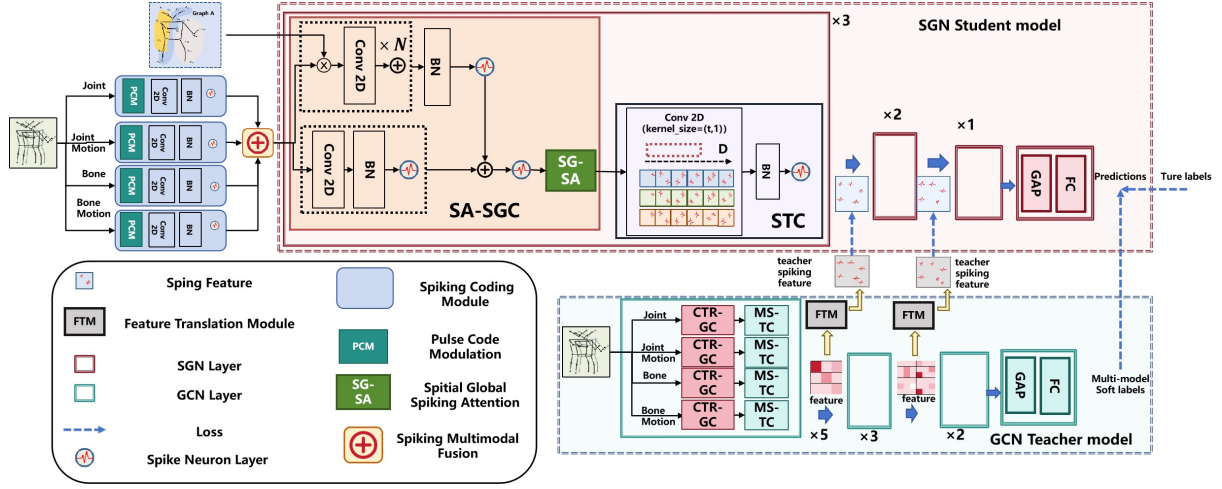


Figure 2: The overview of Spiking Graph Convolutional Network with Multimodal Fusion and Knowledge Distillation (MK-SGN).

aiming to improve accuracy while overlooking energy consumption issues. This work is the first attempt to convert skeleton-based action recognition from ANNs to SNNs, taking the energy consumption issue into full consideration. SNNs differ from ANNs where their information transmission is based on discrete spike sequences rather than continuous floating-point numbers [42], following principles inspired by biology. This operation mode resembles function of human brain and holds significant potential for reducing energy consumption [22]. Early research primarily focused on designing spiking neurons to transform continuous inputs into spike sequences, such as the Leaky Integrate-and-Fire (LIF) neuron [9, 51]. The dynamic model of LIF is described as:

$$\tau_m \frac{dV}{dt} = -(V - V_{\text{rest}}) + R \cdot I(t) \quad (1)$$

In the context of LIF model, $V(t)$ represents the membrane potential at the current time point, where V_{rest} denotes the neuron's resting potential. $I(t)$ indicates the input current. The membrane time constant is given by τ_m , and V_{thresh} is the threshold potential that triggers the firing of an action potential. After firing, the membrane potential is reset to V_{reset} . The model's discrete update time step is Δt . The update of the membrane potential can be written as follows:

$$V(t + \Delta t) = \begin{cases} V_{\text{reset}}, & \text{if } V(t) \geq V_{\text{thresh}} \\ V(t) + \left(\frac{-(V(t) - V_{\text{rest}}) + I(t)}{\tau_m} \right) \Delta t, & \text{otherwise} \end{cases} \quad (2)$$

With the continuous development of ANN frameworks, more research has begun to explore how to utilize existing ANN architectures and weights to design SNNs. Additionally, addressing the differences between backpropagation in spiking networks and ANN has become a key research focus [23, 24, 52]. More studies are devoted to designing ways to replace activation layers in traditional networks with spiking neurons, as events composed of 0s and 1s cannot be used to compute gradients. These studies include Spiking Graph Convolutional Networks (SGCNs) [61], Spiking Transformers [56, 60], Spiking Recurrent Neural Networks (SRNNs) [33] and

Spiking Convolutional Neural Networks (SCNNs) [14, 15]. Existing SNN research involves traditional ANN tasks, with many studies focusing on Transformer models for processing RGB images and achieving significant progress [16, 27]. Some researches concentrate on event-driven recognition [55, 58]. However, research on SNN on skeleton-based action recognition remains relatively scarce.

3 METHODOLOGY

We propose MK-SGN, a novel combination of SNN and GCN for skeleton-based action recognition. First, we introduce a Spiking Coding mechanism to convert skeleton sequence data into spike-form features and propose a Base-SGN network for classification. Then, we present a Spiking Multimodal Fusion module based on mutual information and a spatial spiking graph convolutional network with a spiking attention mechanism. Finally, we propose a multimodal GCN-to-SGN distillation method.

Our network architecture, illustrated in Figure 2, comprises a 10-layer multimodal teacher GCN network [25, 35] and a 6-layer SNN student network. The teacher network predicts the four multimodal skeleton data separately, and the final prediction results are fused after the Global Average Pooling (GAP) and Fully Connected (FC) layers to form soft labels. The student network fuses spike-form feature from multimodal data by mutual information in the Spiking Multimodal Fusion (SMF) module. Each layer of the student network consists of a SA-SGC module and a Spiking Temporal Convolution (STC) module. Our method implements intermediate features and soft label distillation in the knowledge distillation process. The intermediate features of the GCN teacher network are transformed into spike-form feature via the Feature Translation Module (FTM) to guide the training of the student SNN network. More details will be described as follows.

3.1 Skeleton spiking Coding and Base Spiking Graph Convolutional Network (SGN)

In this chapter, we discuss the fundamentals of SNN, focusing on the transformation of continuous real numbers into spike representations. Subsequently, we present Base-SGN, our newly constructed baseline model, which integrates skeleton-based action recognition into the framework of SNN.

3.1.1 Skeleton Spiking Coding. For a given 2D skeleton sequence data $X \in \mathbb{R}^{C \times T \times V}$, we utilize the Spiking Coding (SC) Module to convert it into spike-form features. This module transforms skeleton data with inherent temporal characteristics into a spiking-form representation through linear projection. It maps the temporal window size T and the number of joint nodes V into N -dimensional temporal spiking sequence vector. Meanwhile, it converts the channels into a D -dimensional spike-form feature vector. The whole process can be written as follows:

$$P_0 = \text{PCM}(X) \quad (3)$$

$$P = \text{SN}(\text{BN}(\text{Con2d}(P_0))), P \in \mathbb{R}^{Times \times D \times N} \quad (4)$$

The Pulse Code Modulation module (PCM) converts continuous features into discrete signals and adds a temporal dimension to them. A 2D convolution layer (Conv2d) with kernel size 3, Batch Normalization (BN), and Spiking Neuron layers (SN) aim to achieve deep representation of base signals. At this point, the dimension *Times* no longer represents the original T but rather the temporal dimension of the spiking signals.

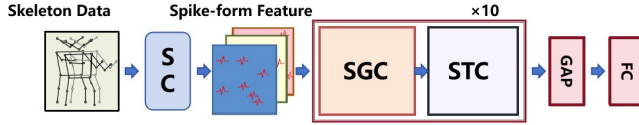


Figure 3: The overflow of Base-SGN

3.1.2 Base-SGN. Revisiting traditional skeleton-based action recognition based on GCN, we now construct our Base-SGN using features converted into the spike-form and adjacency matrices. Its process is illustrated in Figure 3 and can be summarized as follows:

$$S = \tilde{D}^{-\frac{1}{2}} \tilde{A} \tilde{D}^{\frac{1}{2}} \quad (5)$$

where S is the normalized adjacency matrix, $\tilde{A} = A + I$ denotes the sum of the adjacent matrix A and self-connection I . \tilde{D} is the diagonal degree matrix of \tilde{A} . Then, we calculate the graph convolutional output according to the following formula:

$$H = S^K P, H \in \mathbb{R}^{Times \times D \times N} \quad (6)$$

where H represents the output of early spatial spiking graph convolution, K is the number of graph convolutional layers and D is the degree matrix of \tilde{A} . So, the first layer of spatial graph convolution (SGC) can be written as:

$$H_0 = \text{SN}(P) + \text{SN}(HW^{(0)}) \quad (7)$$

where $W^{(0)} \in \mathbb{R}^{D \times D}$ is learnable parameters of the first layer. Each layer has its corresponding learnable weights, which we denote

as $W^{(l)} \in \mathbb{R}^{D^l \times D^{l+1}}$. The first layer of spiking temporal convolution (STC) can be written as:

$$T_0 = \text{SN}(\text{BN}(\text{Con2d}(H_0))) + \text{SN}(H_0) \quad (8)$$

In the Base-SGN, we follow the framework of the traditional GCN, designing a network structure with ten layers. This architecture adopts a "progressive" structure, gradually increasing the channels and adjusting the convolutional stride to prevent overfitting [53]. The complete SGC output H_l and STC output T_l can be written as

$$H_l = \text{SN}(T_{l-1}) + \text{SN}(H_{l-1}W^{(l-1)}) \quad (9)$$

$$T_l = \text{SN}(\text{BN}^{(l)}(\text{Con2d}^{(l)}(H_l))) + \text{SN}(H_l) \quad (10)$$

In the end, the processed feature will be sent to GAP and FC to output the prediction as follows:

$$y = \text{FC}(\text{GAP}(T_l)) \quad (11)$$

where $y \in \mathbb{R}^K$ and K is the number of action classes. Based on this, a standard cross-entropy loss is adopted for model optimization, as formulated as

$$L_b = -\frac{1}{B} \sum_{i=1}^B \sum_{j=1}^K Y_{ij} \log y_{ij} + (1 - Y_{ij}) \log(1 - y_{ij}) \quad (12)$$

where Y is the ground-truth label and B denotes the number of training samples.

3.2 The spiking multimodal fusion module and the spatial graph convolutional network with spiking attention

In this chapter, building upon the SC module and Base-SGN discussed in the previous chapter, we first describe how to fuse multimodal features. Then, we propose a novel SGC with spiking attention.

3.2.1 The spiking multimodal fusion module (SMF). Skeletal data consists of multiple modalities [3], including bones $X_B \in \mathbb{R}^{C \times T \times V}$, joints $X_J \in \mathbb{R}^{C \times T \times V}$ and their motions $X_{BM} \in \mathbb{R}^{C \times T \times V}$, $X_{JM} \in \mathbb{R}^{C \times T \times V}$. As shown in Figure 4, the SMF module implements early fusion based on mutual information to utilize multi-modal data and avoid the additional computing overhead and energy consumption that late fusion causes. In the SMF, we first encode the multimodal data through SC module separately to obtain their spike-form features $P_B \in \mathbb{R}^{Times \times D \times N}$, $P_J \in \mathbb{R}^{Times \times D \times N}$, $P_{BM} \in \mathbb{R}^{Times \times D \times N}$, $P_{JM} \in \mathbb{R}^{Times \times D \times N}$ as Figure 4a. These spike-form features are pairwise selected and concatenated along the dimension D to form a joint distribution. Then, one of the two spikes is randomly shuffled along the temporal dimension *Times*, and the same concatenation is performed to construct a marginal distribution. We employ an LSTM network and fully connected layers to build a mutual information prediction network and calculate the lower bound of mutual information as Figure 4b. We take bone data and joint data as examples, and the process can be described as follows:

$$P_{\text{joint}} = \text{cat}(P_J, P_B, \text{dim} = 1), P_{\text{joint}} \in \mathbb{R}^{Times \times 2D \times N} \quad (13)$$

$$P'_B = P_{\sigma(\text{Times})} \quad (14)$$

$$P_{\text{marginal}} = \text{cat}(P_J, P'_B, \text{dim} = 1), P_{\text{marginal}} \in \mathbb{R}^{Times \times 2D \times N} \quad (15)$$

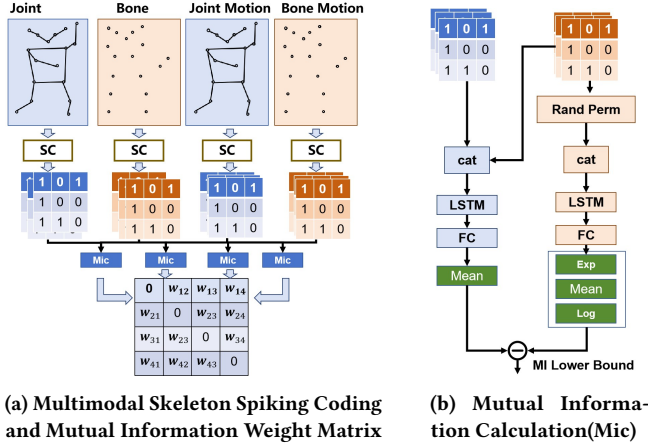


Figure 4: Multimodal Skeleton Spiking Coding and Mutual Information Weight Matrix Calculation Process

$$t = \text{FC}(\text{LSTM}(P_{\text{Joint}})) \quad (16)$$

$$et = \exp\left(\text{FC}\left(\text{LSTM}\left(P_{\text{marginal}}\right)\right)\right) \quad (17)$$

$$mi_lb = \bar{t} - \log \bar{et} \quad (18)$$

Due to the symmetry of mutual information, the mutual information computed pairwise among four groups can be obtained by six calculations, forming a symmetric matrix MI stacked with zeros in the middle. $MI = \begin{bmatrix} 0 & \dots & mi_lb_{jb} \\ \vdots & \ddots & \vdots \\ mi_lb_{bj} & \dots & 0 \end{bmatrix}$. After normaliza-

tion, we obtain the mutual information weight matrix. Multiplying this matrix with the original spike-form features results in the fused features.

$$MI_{av} = \text{sum}(MI, \text{dim} = 1) / \text{sum}(MI) \quad (19)$$

$$W = (MI_{av} - \min MI_{av}) / (\max MI_{av} - \min MI_{av}) \quad (20)$$

$$P_{\text{fuse}} = \text{SA}\left(W * [P_B, P_J, P_{BM}, P_{JM}]^T\right) \quad (21)$$

3.2.2 Spiking Attention Mechanism and Spatial Spiking Graph Convolution. We follow existing spiking attention methods [60], using Conv2d, BN and SN to compute the QKV of the spikes. Due to the differences in backpropagation and gradient calculation between spiking neural networks and traditional neural networks, we avoid using traditional activation functions and softmax to compute attention weight values. Instead, we use QKV with a pure spiking structure through SN and incorporate scaling factors s to control the large value of the matrix multiplication result. The process of computing the corresponding Spiking Attention (SA) using P_{fuse} is as follows:

$$Q = \text{SN}_Q(\text{BN}(PW_Q)), K = \text{SN}_K(\text{BN}(PW_K)) \quad (22)$$

$$V = \text{SN}_V(\text{BN}(PW_V)) \quad (23)$$

$$P_{ssa} = \text{SN}(P_{\text{fuse}}) + \text{SN}(QK^T V * s) \quad (24)$$

Based on the spiking attention mechanism, we propose a Spiking Graph Convolutional Network (SA-SGC) with a spiking attention mechanism built upon the spatial graph convolutional network

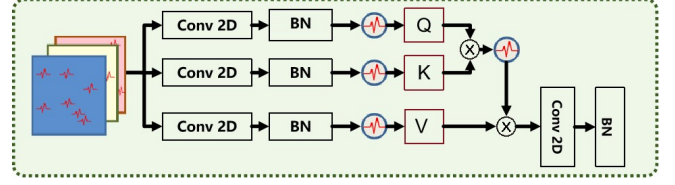


Figure 5: The overview of Spiking Attention

(GC). As illustrated in Figure 2, we integrate the Base-SGN with a spatial global spiking attention mechanism (SGSA). The process of SA-SGC is as follows:

$$H_{SA} = \text{SGSA}\left(P_{ssa} + \bar{D}^{-\frac{1}{2}} \bar{A} \bar{D}^{-\frac{1}{2}} P_{ssa} W\right) \quad (25)$$

In SGSA illustrated in the Figure 5, we first remap the spike-form feature back to $X_{\text{fuse}} \in \mathbb{R}^{C' \times T' \times V'}$, where each dimension C' , T' and V' consists of spiking values over the *Times* dimension, representing a binary spiking pattern of 0 and 1. Subsequently, based on this feature, we compute the global attention mechanism over the T' and V' dimensions. At this point, we compute Q , K and V using spiking values, where each value, similar to SA, consists of 0s and 1s. We then obtain the spatial global attention values by weighting these values. Finally, we remap the values to *Times*, D and N for subsequent STC computation.

3.3 Knowledge Distillation of GCN-to-SGN

To utilize the capabilities of multimodal GCN, we propose a distillation method with GCN as the teacher and SGN as the student. Our method fully exploits the rich knowledge and representation power of pre-trained multimodal GCNs. It enhances the accuracy of the SGN without increasing computational complexity and energy consumption. Additionally, we observe that the SGN trained with teacher model guidance can achieve comparable performance levels even with fewer layers than GCN. Our distillation method includes inner-layer and soft-label distillation as Figure 6.

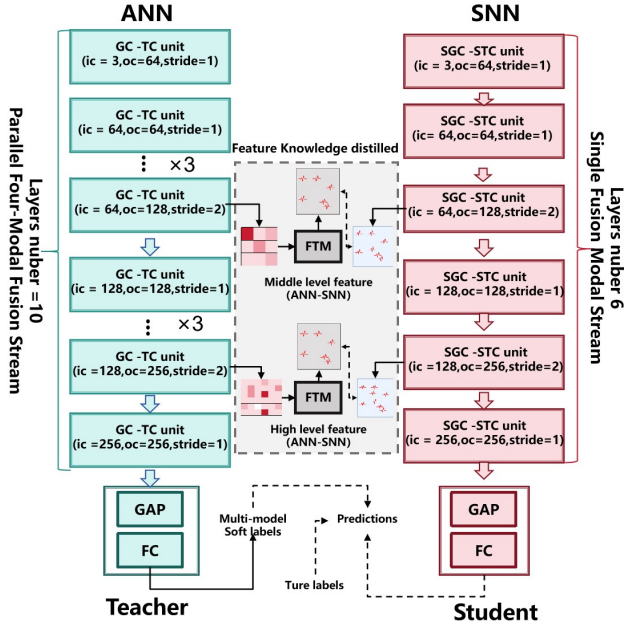
3.3.1 Soft label distillation. For the GCN network, we select a CTR-GCN with a 4-stream structure as the teacher network. In the teacher network, we use skeleton, joint, skeleton-motion and joint-motion data as multi-modal data sources. We input them separately into the single-stream CTR-GCN to obtain single-modal soft labels, denoted as y_b , y_j , y_{bm} and y_{jm} , respectively. Finally, we combine the classification results from each modality to form the multi-modal teacher soft labels \hat{y} .

$$\hat{y} = \alpha_b y_b + \alpha_j y_j + \alpha_{bm} y_{bm} + \alpha_{jm} y_{jm} \quad (26)$$

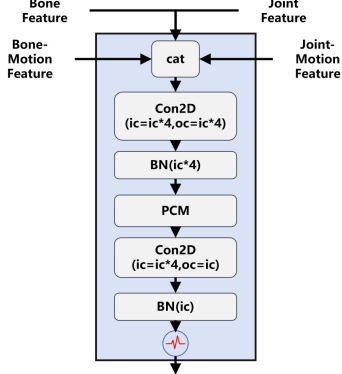
where $\alpha_b, \alpha_j, \alpha_{bm}$ and α_{jm} are hyper-parameters. Then, the final learning objective is written as:

$$L_{sdk} = \|y - \hat{y}\| \quad (27)$$

3.3.2 Inner-layer feature distillation. When considering the inner-layer feature differences between GCN and SGN, it is important to note their distinct approaches to processing input data. GCN typically deals with continuous decimal values, whereas SGN uses discrete spike sequences. We propose FTM designed to effectively convert the continuous inner-layer features of GCN into spike-form features suitable for SGN. We propose the FTM (Feature Translation



(a) Intermediate feature distillation and soft label distillation.



(b) Feature Translation Module

Figure 6: GCN-to-SGN Knowledge Distillation Method

Module), as illustrated in Figure 6b. This module is learnable. Firstly, it concatenates multimodal features along the channel dimension and then fuses them using depth-wise separable convolution. Subsequently, continuous features are encoded using the PCM module. Finally, we employ Conv2D and BN, followed by SN, to obtain spike-form features.

The teacher GCN architecture typically comprises ten GC-TC (Graph Convolution- Temporal Convolution) units. The ic is inter-channel, and the oc is outer-channel. The student GCN architecture typically comprises six units of SGC-STC (Spiking Graph Convolution - Spiking Temporal Convolution). We choose to leverage intermediate-level features $T_{Ab5}, T_{Aj5}, T_{Abm5}, T_{Ajm5} \in \mathbb{R}^{2C \times \frac{T}{2} \times V}$ and high-level features $T_{Ab5}, T_{Aj5}, T_{Abm5}, T_{Ajm5} \in \mathbb{R}^{4C \times \frac{T}{4} \times V}$ as guiding teachers in the learning process. This choice is motivated by the expansion of channel numbers and changes in the TCN

network's stride within these layers. These layers capture diverse temporal relationships and potentially capture richer feature information. We take the intermediate layer as an example, and the process is as follows:

$$T_{Am5} = \text{BN}(\text{Con2d}(\text{cat}(T_{Ab5}, T_{Aj5}, T_{Abm5}, T_{Ajm5}))) \quad (28)$$

where $T_{Am5} \in \mathbb{R}^{8C \times \frac{T}{2} \times V}$ are fused multi-modal teacher features.

$$T_{Am5} = \text{SN}(\text{BN}(\text{Con2d}(\text{PCM}(T_{Am5})))) \quad (29)$$

, where $T_{Sm5} \in \mathbb{R}^{\text{Times} \times 2D \times \frac{N}{2}}$ are teacher spike-form feature. Similarly, we calculate the spike-form feature for the high-level layer $T_{Sm8} \in \mathbb{R}^{\text{Times} \times 4D \times \frac{N}{4}}$. To guide the student network with the teacher's pulse features, we employ cosine similarity as the loss function to measure the discrepancy between each pair of feature vectors.

$$L_{\text{fkd}_1} = \frac{1}{K} \sum_{i=1}^K \left(1 - \frac{T_{Sm5}^i \cdot S_3^i}{\|T_{Sm5}^i\| \cdot \|S_3^i\|} \right) \quad (30)$$

$$L_{\text{fkd}_2} = \frac{1}{K} \sum_{i=1}^K \left(1 - \frac{T_{Sm8}^i \cdot S_8^i}{\|T_{Sm8}^i\| \cdot \|S_8^i\|} \right) \quad (31)$$

$S_3 \in \mathbb{R}^{\text{Times} \times 2D \times \frac{N}{2}}$ are the spike-form feature of the 3th lay of SGN and $S_5 \in \mathbb{R}^{\text{Times} \times 4D \times \frac{N}{4}}$ are the 5th. K is the number of action classes. And inner-layer feature distillation loss is written as:

$$L_{\text{fkd}} = \beta_1 L_{\text{fkd}_1} + \beta_2 L_{\text{fkd}_2} \quad (32)$$

where β_1 and β_2 are hyper-parameters. This aims to drive the student network features closer to the teacher features while optimizing the FTM for feature translation. In the end, the final learning objective with hyper-parameters γ_1, γ_2 and γ_3 is re-written as

$$L = \gamma_1 L_b + \gamma_2 L_{\text{sdk}} + \gamma_3 L_{\text{fkd}} \quad (33)$$

4 EXPERIMENTS

4.1 Datasets

NTU-RGB+D 60: It is a widely used dataset for skeleton-based action recognition research [38]. It comprises 60 action categories with 56,880 skeleton sequences, each containing 25 joints. The data is sourced from 40 subjects and captured using three cameras at various angles to ensure diverse action capture. Two evaluation protocols are employed: Cross-Subject (X-sub) and Cross-View (X-view). In X-sub, 20 subjects are used for training and another 20 for testing, while in X-view, samples from one camera are used for testing and the rest for training, simulating different perspectives for action recognition.

NTU-RGB+D 120: It extends NTU-RGB+D 60, providing researchers with more prosperous and more diverse data resources [28]. In addition to expanding to 120 action categories, the dataset also increases the number of skeleton sequences to 114,480. It includes action samples from 106 unique subjects captured from 155 view-points and three camera perspectives. To simulate real-world action recognition scenarios more effectively, the dataset offers 32 different setups, each representing unique locations and backgrounds. Skeleton data consists of 3D coordinates for 25 joints, providing detailed and accurate action descriptions. Evaluation benchmarks

Table 1: Evaluation on NTU-RGB+D. Param refers to the number of parameters. Power is the average theoretical energy consumption when predicting a skeleton from the NTU-RGB+D test set, whose calculation details are shown as Equation(35), Equation(36) and Equation(37).

Method	Architecture	Param (M)	Time Step	Modal Number	Knowledge Distillation	OPs (G)	Power (mJ)	Ntu-RGB+D 60 XSub(%)	XView(%)
ANN	ST-GCN(Baseline) [53]	2.11	/	1	/	2.56	11.78	81.5	88.3
	Base-SGN	2.07	4	1	/	0.60	5.36×10^{-1}	64.2	71.3
SNN	(10-layer) MK-SGN	3.13	4	1	/	0.96	8.60×10^{-1}	72.9	79.6
	(10-layer) MK-SGN	3.13	4	1	✓	0.98	8.78×10^{-1}	74.3	81.2
	(10-layer) MK-SGN	3.24	4	4	/	1.00	9.12×10^{-1}	74.2	80.1
	(10-layer) MK-SGN	3.24	4	4	✓	1.02	9.31×10^{-1}	78.2	85.1
	(6-layer) MK-SGN	1.89	4	1	/	0.64	5.73×10^{-1}	72.1	78.9
	(6-layer) MK-SGN	1.89	4	1	✓	0.66	5.82×10^{-1}	74.9	82.1
	(6-layer) MK-SGN	2.17	4	4	/	0.67	5.98×10^{-1}	74.1	79.8
	(6-layer) MK-SGN	2.17	4	4	✓	0.68	6.14×10^{-1}	78.5	85.6

include not only Cross-Subject (X-Sub) but also introduce Cross-Setup (X-Set), assessing algorithms' generalization across different scenarios.

4.2 Implementation Details

The models for conducting experiments are implemented based on Pytorch [36] and SpikingJelly [11] on a server equipped with an NVIDIA SMI V100 GPU, which has 30GB of memory. We adopt the SGD optimizer with a learning rate of 0.02 and a weight decay rate of 0.02 for efficient parameter optimization of Base-SGN. The batch size is set to 60 for NTU-RGB+D 60 and 40 for NTU-RGB+D 120. We employ two SGD optimizers during our training process to fine-tune MK-SGN parameters. One optimizer is specifically used to enhance the SGN model, improving its efficiency in handling tasks; the other optimizer is dedicated to refining the FTM, boosting the effectiveness of feature transfer from the teacher to the student model. In the testing phase, we only evaluate the SGN model itself.

4.3 Theoretical Energy Consumption Calculation

Referencing [60], we must first calculate the synaptic operations when calculating theoretical energy consumption. Then, according to [20, 21, 57], the theoretical energy consumption of Base-SGN and MK-SGN are calculated as:

$$\text{SOPs}(l) = fr \times \text{Times} \times \text{FLOPs}(l) \quad (34)$$

$$E_{\text{Base-SGN}} = E_{\text{MAC}} \times \text{FL}_{\text{SNNConv}}^1 + E_{\text{AC}} \times \left(\sum_{n=2}^N \text{SOP}_{\text{SNNConv}}^n + \sum_{m=1}^M \text{SOP}_{\text{SNNFC}}^m \right) \quad (35)$$

$$E_{\text{MK-SGN}} = n_m \times E_{\text{MAC}} \times \text{FL}_{\text{SNNConv}}^1 + E_{\text{AC}} \times \left(\left[\frac{k \times (k-1)}{2} \right] \text{SOP}_{\text{Mc}} + \sum_{n=n_m}^N \text{SOP}_{\text{SNNConv}}^n + \sum_{m=1}^M \text{SOP}_{\text{SNNFC}}^m + \sum_{l=1}^L \text{SOP}_{\text{SA}}^l + \sum_{i=1}^I \text{SOP}_{\text{SGSA}}^i \right) \quad (36)$$

where l is a block/layer in SGN, fr is the firing rate of the input spike train of the block/layer and Times is the simulation time step of the spiking neuron. $\text{FLOPs}(l)$ refers to the floating point operations of l , which is the number of multiply-and-accumulate (MAC) operations. And SOPs is the number of spike-based accumulate (AC) operations. FL_{SNN}^1 is the first layer to encode skeleton data into spike-form. The SOP of n SNN Conv layers, m SNN Fully Connected Layer (FC) and l SA and i SGSA are added together and multiplied by E_{MAC} . When calculating $E_{\text{MK-SGN}}$, SOP_{Mc} is utilized to estimate the theoretical energy consumption of fusing k modalities. We assume that the MAC and AC operations are implemented on the 45nm hardware [60], where $E_{\text{MAC}} = 4.6pJ$ and $E_{\text{AC}} = 0.9pJ$. The theoretical energy consumption of block b for ANN and SNN are as follows:

$$\text{Power}(b) = 4.6pJ \times \text{FLOPs}(b) \quad (37)$$

$$\text{Power}(b) = 0.9pJ \times \text{SOPs}(b) \quad (38)$$

4.4 Ablation Study

To analyze the energy efficiency of our proposed Base-SGN and further assess the effectiveness of each component in the MK-SGN network, we employ theoretical formulas to evaluate the number of operations (OPs) required for classifying a single sample. Specifically, we calculate ANN's number of floating-point operations (FLOPs) and SNN's theoretical number of synaptic operations (SOPs) Based on these OPs, we further calculate the energy consumption per action sample during the testing phase. Lastly, we

analyze the classification accuracy through all experimental ablation studies conducted on the NTU RGB+D 60 dataset, as shown in Table 1.

4.4.1 Base-SGN. First, we validate the energy efficiency of the Base-SGN proposed in Section 3.1.2. To demonstrate the potential of our newly proposed network in significantly reducing energy consumption while maintaining a certain level of classification accuracy, we use the trained model and compare it with the traditional ST-GCN. We calculate theoretical OPs and energy consumption. The results show that Base-SGN reduces OPs and theoretical energy consumption by $0.536mJ$ per action sample, while certain degrees of accuracy, 64.2% and 71.3%, are preserved.

4.4.2 SA-SGC. On the foundation of Base-SGN, we compare the impact of incorporating the SA-SGC module. We evaluate the accuracy of the SGN with the module integrated compared to the Base-SGN, as well as their OPs and Power. SA-SGC increases the OPs and theoretical Power and significantly improves accuracy by 10.1% and 8.9% for skeleton action classification based on SGNs.

4.4.3 SMF. In the case of late fusion in a multi-modal classification network, where n represents the number of modalities when classifying a single action sample, it must undergo testing for n times, leading to a theoretical energy consumption expanded to n times the original. Taking ST-GCN as an example, its theoretical OPs will become $4 \times 2.56G$ and the Power will become $4 \times 11.78mJ$. To validate that our designed SMF can avoid the increased energy consumption caused by late fusion and improve accuracy, we compare the performance of multi-modal fusion with single-modal fusion. This approach avoids the increased energy consumption caused by late fusion. The theoretical energy consumption only increased by $0.62mJ$ per action sample. And it improves the model's accuracy by 0.1% and 0.5%

4.4.4 Knowledge Distillation. We compare the accuracy of models trained with and without teacher guidance. We observe their OPs and Power to evaluate the impact of our proposed knowledge distillation method. The accuracy of SGN models trained with teacher guidance shows a noticeable improvement of 4.0% and 4.5%. At the same time, OPs and Power exhibit slight fluctuations (due to differences in the firing rates of spiking neural networks), with no significant increase observed.

4.4.5 Layer Reduction and Contribution of each Component. We first discuss whether reducing the layers of SGN will affect the accuracy. Simplifying the model's layers reduces computational load and energy consumption by over 30%. It leads to a slight decrease in model accuracy. This effectively compensates for the precision loss caused by the reduction of layers and further improves the model's accuracy. We find that under the guidance of the teacher model, SGN shows remarkable potential. Compared with the 10-layer SGN, the OPs and Power of the 6-layer SGN decrease significantly. The 6-layer SGN stands at 0.68 GOPs and power consumption at $0.614mJ$ per action sample. Then, we scrutinise the contribution of each MK-SGN component as shown in Table 1.

4.5 Experimental Results

We compare our proposed SGN approach with the current state-of-the-art (SOTA) ANNs. We particularly focus on two key performance metrics: the number of operations (OPs) and the theoretical energy consumption—in Table. 2 and Table. 3. To make fair comparisons, in both tables, the results of existing multi-modal GCN methods of four modalities, i.e., joint, bone, joint motion, and bone motion, are fused. The softmax scores of multiple streams are added to obtain the fused score. Their Ops and theoretical energy consumption are calculated by multiplying the corresponding value of a single flow by the number of modal flows.

Table 2: Comparative results on NTU RGB+D 60. We evaluate our model in terms of classification accuracy (%). X-Sub and X-view represent cross-subject and cross-view

Method	Architecture	Param (M)	OPs (G)	Power (mJ)	Xsub (%)	Xview (%)
ANN	Lie Group [47]	/	/	/	50.1	52.8
	HBRMM [8]	/	/	/	59.1	64.0
	Deep LSTM [38]	/	/	/	60.7	67.3
	TCN [44]	/	/	/	74.3	83.1
	ST-GCN [53]	2.11	2.56	11.78	81.5	88.3
	2S-AGCN [41]	3.48	35.8	164.68	89.2	95.0
	Shift-GCN [5]	/	10	46	90.7	96.5
	MS-G3D [17]	3.19	67.63	311.09	91.5	96.2
	CTR-GCN [3]	1.46	7.88	36.25	92.4	96.8
SNN	Base-SGN	2.07	0.60	5.36×10^{-1}	64.2	71.3
	MK-SGN	2.17	0.68	6.14×10^{-1}	78.5	85.6

Table 3: Comparative results on NTU RGB+D 120. We evaluate our model in terms of classification accuracy (%). X-Sub and X-Set represent cross-subject and cross-setup splits

Method	Architecture	Param (M)	OPs (G)	Power (mJ)	Xsub (%)	Xview (%)
ANN	Part-Aware LSTM [38]	/	/	/	25.5	26.3
	ST-LSTM [29]	/	/	/	55.7	57.9
	Multi CNN + RotClips [17]	/	/	/	61.8	62.2
	SkeMotion [30]	/	/	/	66.9	67.7
	SGN [59]	/	/	/	62.8	67.9
	2S-AGCN [41]	3.48	35.8	165.68	82.9	84.9
	Shift-GCN [5]	/	10	46	85.9	87.6
	MS-G3D [32]	3.19	67.63	311.09	86.9	88.4
	CTR-GCN [3]	1.46	7.88	36.25	88.9	90.6
SNN	Base-SGN	2.07	0.60	5.36×10^{-1}	45.2	47.3
	MK-SGN	2.17	0.68	6.14×10^{-1}	67.8	69.5

We report the results of the 6-layer MK-SGN. MK-SGN achieves significantly higher accuracy on the NTU RGB+D 60 dataset than previous non-GCN ANN models [8, 38, 44, 47]. It also achieves higher accuracy on the NTU RGB+D 120 dataset than non-GCN ANN models [17, 29, 30, 38, 59]. Its theoretical energy consumption is $0.614mJ$ per action sample. Compared with the 2s-AGCN method [41], the theoretical energy consumption is reduced by 99.62%. Compared with MS-G3D, the theoretical energy consumption is reduced by 99.80%. Compared with Shift-GCN[5] and CTR-GCN [3], which are characterized by lightweight, the theoretical energy consumption is reduced by 98.67% and 98.31%, respectively.

These results empirically verify the advantage of MK-SGN in skeleton-based action recognition.

5 CONCLUSION

This work introduces a Spiking Graph Convolutional Network with Multimodal Fusion and Knowledge Distillation (MK-SGN). This is the first time that spiking neural networks and graph convolutional networks have been combined with multimodal fusion and knowledge distillation for skeleton action recognition. Our research overcomes the problem of traditional GCN-based methods' large energy consumption and achieves significant performance improvements.

On the two datasets of skeleton-based action recognition, the MK-SGN model significantly outperformed the current state-of-the-art methods in reducing energy consumption, with 0.614mJ per action sample. It reduces energy consumption by more than 98%.

This achievement demonstrates our model's efficiency and performance advantages and offers a new direction for future low-energy, high-efficiency intelligent systems. Future research will delve further into the impact of hierarchical and network structures on model accuracy and how to find the optimal balance between the model's energy consumption and accuracy. We plan to explore different network architectures and multimodal fusion strategies to optimize the SGN model, enabling it to perform effectively in various application areas.

REFERENCES

- Agapios Agapiou, Anton Amann, Pawel Mochalski, Milt Statheropoulos, and Charles Lawrence Paul Thomas. 2015. Trace detection of endogenous human volatile organic compounds for search, rescue and emergency applications. *TrAC Trends in Analytical Chemistry* 66 (2015), 158–175.
- Tadas Baltrušaitis, Chaitanya Ahuja, and Louis-Philippe Morency. 2018. Multimodal machine learning: A survey and taxonomy. *IEEE transactions on pattern analysis and machine intelligence* 41, 2 (2018), 423–443.
- Yuxin Chen, Ziqi Zhang, Chunfeng Yuan, Bing Li, Ying Deng, and Weiming Hu. 2021. Channel-wise topology refinement graph convolution for skeleton-based action recognition. (2021), 13359–13368.
- Zhan Chen, Sicheng Li, Bing Yang, Qinghan Li, and Hong Liu. 2021. Multi-scale spatial temporal graph convolutional network for skeleton-based action recognition. 35, 2 (2021), 1113–1122.
- Ke Cheng, Yifan Zhang, Xiangyu He, Weihai Chen, Jian Cheng, and Hanqing Lu. 2020. Skeleton-based action recognition with shift graph convolutional network. (2020), 183–192.
- Guilhem Chéron, Ivan Laptev, and Cordelia Schmid. 2015. P-cnn: Pose-based cnn features for action recognition. (2015), 3218–3226.
- Hyung-gun Chi, Myoung Hoon Ha, Seunggeun Chi, Sang Wan Lee, Qixing Huang, and Karthik Ramani. 2022. Infocnn: Representation learning for human skeleton-based action recognition. (2022), 20186–20196.
- Yong Du, Wei Wang, and Liang Wang. 2015. Hierarchical recurrent neural network for skeleton based action recognition. (2015), 1110–1118.
- Sangya Dutta, Vinay Kumar, Aditya Shukla, Nihar R Mohapatra, and Udayan Ganguly. 2017. Leaky integrate and fire neuron by charge-discharge dynamics in floating-body MOSFET. *Scientific reports* 7, 1 (2017), 8257.
- Omar Elharrouss, Noor Almaadeed, and Somaya Al-Maadeed. 2021. A review of video surveillance systems. *Journal of Visual Communication and Image Representation* 77 (2021), 103116.
- Wei Fang, Yanqi Chen, Jianhao Ding, Zhaofei Yu, Timothée Masquelier, Ding Chen, Liwei Huang, Huihui Zhou, Guoqi Li, and Yonghong Tian. 2023. Spiking-Jelly: An open-source machine learning infrastructure platform for spike-based intelligence. *Science Advances* 9, 40 (2023), eadi1480.
- Liqi Feng, Yaqin Zhao, Wenxuan Zhao, and Jiayi Tang. 2022. A comparative review of graph convolutional networks for human skeleton-based action recognition. *Artificial Intelligence Review* (2022), 1–31.
- Jing Gao, Peng Li, Zhikui Chen, and Jianing Zhang. 2020. A survey on deep learning for multimodal data fusion. *Neural Computation* 32, 5 (2020), 829–864.
- Yifan Hu, Lei Deng, Yujie Wu, Man Yao, and Guoqi Li. 2024. Advancing Spiking Neural Networks Toward Deep Residual Learning. *IEEE Transactions on Neural Networks and Learning Systems* (2024).
- Yangfan Hu, Huajin Tang, and Gang Pan. 2021. Spiking deep residual networks. *IEEE Transactions on Neural Networks and Learning Systems* 34, 8 (2021), 5200–5205.
- Yangfan Hu, Qian Zheng, Xudong Jiang, and Gang Pan. 2023. Fast-snn: Fast spiking neural network by converting quantized ann. *IEEE Transactions on Pattern Analysis and Machine Intelligence* (2023).
- Qihong Ke, Mohammed Bennamoun, Senjian An, Ferdous Sohel, and Farid Bousaid. 2018. Learning clip representations for skeleton-based 3d action recognition. *IEEE Transactions on Image Processing* 27, 6 (2018), 2842–2855.
- Hyunjik Kim and Andriy Mnih. 2018. Disentangling by factorising. (2018), 2649–2658.
- Youngeun Kim, Joshua Chough, and Priyadarshini Panda. 2022. Beyond classification: Directly training spiking neural networks for semantic segmentation. *Neuromorphic Computing and Engineering* 2, 4 (2022), 044015.
- Souvik Kundu, Gourav Datta, Massoud Pedram, and Peter A Beerel. 2021. Spike-thrift: Towards energy-efficient deep spiking neural networks by limiting spiking activity via attention-guided compression. In *Proceedings of the IEEE/CVF Winter Conference on Applications of Computer Vision*. 3953–3962.
- Souvik Kundu, Massoud Pedram, and Peter A Beerel. 2021. Hire-snn: Harnessing the inherent robustness of energy-efficient deep spiking neural networks by training with crafted input noise. In *Proceedings of the IEEE/CVF International Conference on Computer Vision*. 5209–5218.
- Chankyu Lee, Syed Shakib Sarwar, Priyadarshini Panda, Gopalakrishnan Srivasan, and Kaushik Roy. 2020. Enabling spike-based backpropagation for training deep neural network architectures. *Frontiers in neuroscience* 14 (2020), 497482.
- Chankyu Lee, Syed Shakib Sarwar, Priyadarshini Panda, Gopalakrishnan Srivasan, and Kaushik Roy. 2020. Enabling spike-based backpropagation for training deep neural network architectures. *Frontiers in neuroscience* 14 (2020), 497482.
- Jun Haeng Lee, Tobi Delbruck, and Michael Pfeiffer. 2016. Training deep spiking neural networks using backpropagation. *Frontiers in neuroscience* 10 (2016), 228000.
- Bin Li, Xi Li, Zhongfei Zhang, and Fei Wu. 2019. Spatio-temporal graph routing for skeleton-based action recognition. 33, 01 (2019), 8561–8568.
- Maosen Li, Siheng Chen, Xu Chen, Ya Zhang, Yanfeng Wang, and Qi Tian. 2019. Actional-structural graph convolutional networks for skeleton-based action recognition. (2019), 3595–3603.
- Yihan Lin, Yifan Hu, Shijie Ma, Dongjie Yu, and Guoqi Li. 2022. Rethinking pretraining as a bridge from anns to snns. *IEEE Transactions on Neural Networks and Learning Systems* (2022).
- Jun Liu, Amir Shahroudy, Mauricio Perez, Gang Wang, Ling-Yu Duan, and Alex C Kot. 2019. Ntu rgb+ d 120: A large-scale benchmark for 3d human activity understanding. *IEEE transactions on pattern analysis and machine intelligence* 42, 10 (2019), 2684–2701.
- Jun Liu, Amir Shahroudy, Dong Xu, and Gang Wang. 2016. Spatio-temporal lstm with trust gates for 3d human action recognition. In *Computer Vision—ECCV 2016: 14th European Conference, Amsterdam, The Netherlands, October 11–14, 2016, Proceedings, Part III 14*. Springer, 816–833.
- Jun Liu, Gang Wang, Ping Hu, Ling-Yu Duan, and Alex C Kot. 2017. Global context-aware attention lstm networks for 3d action recognition. (2017), 1647–1656.
- Mengyuan Liu, Hong Liu, and Chen Chen. 2017. Enhanced skeleton visualization for view invariant human action recognition. *Pattern Recognition* 68 (2017), 346–362.
- Ziyu Liu, Hongwen Zhang, Zhenghao Chen, Zhiyong Wang, and Wanli Ouyang. 2020. Disentangling and unifying graph convolutions for skeleton-based action recognition. (2020), 143–152.
- Ali Lotfi Rezaabad and Sriram Vishwanath. 2020. Long short-term memory spiking networks and their applications. (2020), 1–9.
- Wolfgang Maass. 1997. Networks of spiking neurons: the third generation of neural network models. *Neural networks* 10, 9 (1997), 1659–1671.
- Cosmas Ifeanyi Nwakanma, Fableda Bushra Islam, Mareska Pratiwi Maharani, Dong-Seong Kim, and Jae-Min Lee. 2021. Iot-based vibration sensor data collection and emergency detection classification using long short term memory (lstm). (2021), 273–278.
- Adam Paszke, Sam Gross, Francisco Massa, Adam Lerer, James Bradbury, Gregory Chanan, Trevor Killeen, Zeming Lin, Natalia Gimelshein, Luca Antiga, et al. 2019. Pytorch: An imperative style, high-performance deep learning library. *Advances in neural information processing systems* 32 (2019).
- Kaushik Roy, Akhilesh Jaiswal, and Priyadarshini Panda. 2019. Towards spike-based machine intelligence with neuromorphic computing. *Nature* 575, 7784 (2019), 607–617.
- Amir Shahroudy, Jun Liu, Tian-Tsong Ng, and Gang Wang. 2016. Ntu rgb+ d: A large scale dataset for 3d human activity analysis. (2016), 1010–1019.
- Thomas B Sheridan. 2016. Human-robot interaction: status and challenges. *Human factors* 58, 4 (2016), 525–532.
- Lei Shi, Yifan Zhang, Jian Cheng, and Hanqing Lu. 2019. Skeleton-based action recognition with directed graph neural networks. (2019), 7912–7921.
- Lei Shi, Yifan Zhang, Jian Cheng, and Hanqing Lu. 2019. Two-stream adaptive graph convolutional networks for skeleton-based action recognition. In *Proceedings of the IEEE/CVF conference on computer vision and pattern recognition*. 12026–12035.

- [42] Sumit B Shrestha and Garrick Orchard. 2018. Slayer: Spike layer error reassignment in time. *Advances in neural information processing systems* 31 (2018).
- [43] Sijie Song, Cuiling Lan, Junliang Xing, Wenjun Zeng, and Jiaying Liu. 2017. An end-to-end spatio-temporal attention model for human action recognition from skeleton data. In *Proceedings of the AAAI conference on artificial intelligence*, Vol. 31.
- [44] Tae Soo Kim and Austin Reiter. 2017. Interpretable 3d human action analysis with temporal convolutional networks. In *Proceedings of the IEEE conference on computer vision and pattern recognition workshops*. 20–28.
- [45] Evangelos Stamatias, Miguel Soto, Teresa Serrano-Gotarredona, and Bernabé Linares-Barranco. 2017. An event-driven classifier for spiking neural networks fed with synthetic or dynamic vision sensor data. *Frontiers in neuroscience* 11 (2017), 269013.
- [46] Amirhossein Tavanaei, Masoud Ghodrati, Saeed Reza Kheradpisheh, Timothée Masquelier, and Anthony Maida. 2019. Deep learning in spiking neural networks. *Neural networks* 111 (2019), 47–63.
- [47] Vivek Veeriah, Naifan Zhuang, and Guo-Jun Qi. 2015. Differential recurrent neural networks for action recognition. (2015), 4041–4049.
- [48] Michalis Vrigkas, Christophoros Nikou, and Ioannis A Kakadiaris. 2015. A review of human activity recognition methods. *Frontiers in Robotics and AI* 2 (2015), 28.
- [49] Hongsong Wang and Liang Wang. 2017. Modeling temporal dynamics and spatial configurations of actions using two-stream recurrent neural networks. (2017), 499–508.
- [50] Yizhou Wang, Yixuan Wu, Shixiang Tang, Weizhen He, Xun Guo, Feng Zhu, Lei Bai, Rui Zhao, Jian Wu, Tong He, et al. 2023. Hulk: A Universal Knowledge Translator for Human-Centric Tasks. *arXiv preprint arXiv:2312.01697* (2023).
- [51] Yujie Wu, Lei Deng, Guoqi Li, and Luping Shi. 2018. Spatio-temporal backpropagation for training high-performance spiking neural networks. *Frontiers in neuroscience* 12 (2018), 323875.
- [52] Mingqing Xiao, Qingyan Meng, Zongpeng Zhang, Yisen Wang, and Zhouchen Lin. 2021. Training feedback spiking neural networks by implicit differentiation on the equilibrium state. *Advances in neural information processing systems* 34 (2021), 14516–14528.
- [53] Sijie Yan, Yuanjun Xiong, and Dahua Lin. 2018. Spatial temporal graph convolutional networks for skeleton-based action recognition. In *Proceedings of the AAAI conference on artificial intelligence*, Vol. 32.
- [54] Sen Yang, Xuanhan Wang, Lianli Gao, and Jingkuan Song. 2022. Mke-gcn: Multimodal knowledge embedded graph convolutional network for skeleton-based action recognition in the wild. In *2022 IEEE International Conference on Multimedia and Expo (ICME)*. IEEE, 01–06.
- [55] Man Yao, Huanhuan Gao, Guangshe Zhao, Dingheng Wang, Yihan Lin, Zhaoxu Yang, and Guoqi Li. 2021. Temporal-wise attention spiking neural networks for event streams classification. In *Proceedings of the IEEE/CVF International Conference on Computer Vision*. 10221–10230.
- [56] Man Yao, Jiakui Hu, Zhaokun Zhou, Li Yuan, Yonghong Tian, Bo Xu, and Guoqi Li. 2024. Spike-driven transformer. *Advances in Neural Information Processing Systems* 36 (2024).
- [57] Man Yao, Guangshe Zhao, Hengyu Zhang, Yifan Hu, Lei Deng, Yonghong Tian, Bo Xu, and Guoqi Li. 2023. Attention spiking neural networks. *IEEE transactions on pattern analysis and machine intelligence* (2023).
- [58] Jiqing Zhang, Bo Dong, Haiwei Zhang, Jianchuan Ding, Felix Heide, Baocai Yin, and Xin Yang. 2022. Spiking transformers for event-based single object tracking. (2022), 8801–8810.
- [59] Pengfei Zhang, Cuiling Lan, Wenjun Zeng, Junliang Xing, Jianru Xue, and Nan-ning Zheng. 2020. Semantics-guided neural networks for efficient skeleton-based human action recognition. In *proceedings of the IEEE/CVF conference on computer vision and pattern recognition*. 1112–1121.
- [60] Zhaokun Zhou, Yuesheng Zhu, Chao He, Yaowei Wang, Shuicheng Yan, Yonghong Tian, and Li Yuan. 2022. Spikformer: When spiking neural network meets transformer. *arXiv preprint arXiv:2209.15425* (2022).
- [61] Zulun Zhu, Jiaying Peng, Jintang Li, Liang Chen, Qi Yu, and Siqiang Luo. 2022. Spiking graph convolutional networks. *arXiv preprint arXiv:2205.02767* (2022).